Performance Analysis of Energy Detection for MIMO Decision Fusion in Wireless Sensor Networks Over Arbitrary Fading Channels

Pierluigi Salvo Rossi, *Senior Member, IEEE*, Domenico Ciuonzo, *Senior Member, IEEE*, Kimmo Kansanen, *Member, IEEE*, and Torbjörn Ekman, *Member, IEEE*

***Abstract*— In this paper, we consider a wireless sensor network (WSN) with sensors simultaneously reporting their decision to a fusion center (FC) equipped with multiple antennas. A Gaussian mixture channel model is used to obtain a general fading characterization of the channels ensemble between the sensors and the FC. Energy detection is studied as an appealing low-complexity sub-optimal alternative to the (computationally expensive) optimal test based on log-likelihood ratio. Closed-form theoretical performance is obtained for the energy test and furthermore asymptotic analysis for both tests is derived in order to provide a detailed characterization of large-system scenarios. Finally, the simulation results are provided to confirm the theoretical results and compare performance trends of the two tests.**

***Index Terms*— Decision fusion, energy detection, Gaussian mixture (GM), multiple-input multiple-output (MIMO), wireless sensor network (WSN).**

I. Introduction

Wireless sensor networks (WSNs) have been studied extensively in various research contexts. Among the relevant problems, distributed detection represents a task of interest in many applications, ranging from surveillance and air-traffic control, to aquaculture and oil exploration [1]. Due to severe bandwidth and energy limitations on the network, each sensor node usually compresses its observations in the form of a local decision related to the underlying phenomenon, which is then exchanged throughout the network in order to obtain robust detection regarding events of interest. The aforementioned problem is usually referred to as "decision fusion".

Manuscript received June 15, 2016; revised August 27, 2016; accepted September 5, 2016. Date of publication September 8, 2016; date of current version November 9, 2016. This work was supported in part by the ERCIM within the Alain Bensoussan Fellowship Programme and in part by the Faculty of Information Technology, Mathematics and Electrical Engineering of the Norwegian University of Science and Technology, Trondheim, Norway, within the Project CAMOS. The associate editor coordinating the review of this paper and approving it for publication was A. Maaref.

P. Salvo Rossi, K. Kansanen, and T. Ekman are with the Department of Electronics and Telecommunications, Norwegian University of Science and Technology, 7491 Trondheim, Norway (e-mail: salvorossi@ieee.org; kimmo.kansanen@iet.ntnu.no; torbjorn.ekman@iet.ntnu.no).

D. Ciuonzo is with the Department of Electrical Engineering and Information Technology, University of Naples Federico II, 80138 Naples, Italy. This work was performed while he was visiting the Department of Electronics and Telecommunications, Norwegian University of Science and Technology, Trondheim, Norway (e-mail: domenico.ciuonzo@ieee.org).

Color versions of one or more of the figures in this paper are available online at http://ieeexplore.ieee.org.

Digital Object Identifier 10.1109/TWC.2016.2607703

A. Related Work

Two architectures have been typically investigated: (i) *centralized* [2], in which the sensors transmit their local decisions to a fusion center (FC) which takes a (more reliable) global decision by appropriately combining the received information; (ii) *decentralized* [3], in which there is no FC and each sensor collects the information from the remaining ones in order to reach autonomously a reliable decision.

Focusing on centralized architectures, they have been commonly based on a parallel access channel (PAC), where each sensor is provided with a non-interfering dedicated (i.e. orthogonal to the others) channel to communicate with the FC [4]. Orthogonality is commonly achieved via frequency or time division multiple-access techniques. Unfortunately, the PAC assumption implies a large bandwidth requirement for simultaneous transmissions or a large detection delay, which is unfeasible for large-scale sensor networks unless sensor selection is employed [5]. Channel state information (CSI) available at the FC has been exploited in the case of PAC for design and analysis of near-optimal fusion rules [6], while use of differential modulation is investigated in [7].

Recently, the intrinsically interfering nature of the wireless medium has been exploited in the context distributed detection. PAC assumption has been replaced with multiple access channel (MAC) for bandwidth efficiency [8], [9] and the advantage of multiple antennas at the FC has been analyzed in terms of error exponent in [10]. Looking at the network as a "virtual" multi-input multi-output (MIMO) system, array processing techniques at the FC have been investigated and compared in terms of performance, complexity, and knowledge requirements in [11]. Maximum ratio combining has been investigated in detail in [12] as an appealing technique exhibiting excellent performance with limited complexity. The impact of massive MIMO, i.e. a very-large array at the FC, has been evaluated in [13] where low-complexity solutions designed on a PAC assumption are shown to be asymptotically optimum in MAC scenarios.

It is worth noticing that all these works rely on instantaneous CSI for design of fusion rule at the FC. Unfortunately, in some relevant scenarios such as anomaly detection, instantaneous CSI acquisition may be too costly from an energy point of view. In such a case, on-off keying (OOK) represents an advantageous modulation which complies with statistical CSI and also ensures implicit nearly-optimal censoring policy [14], i.e. additional energy saving. In this scenario, energy detection at the FC was proven to be optimal in Rayleigh fading channels [15] and near-optimal in *non-line-of-sight* fading channels [16], thus constituting an attractive candidate at FC design stage, and further explored in [17] for suitability in underwater WSNs and in [18] with a focus on Bayesian modeling.

In this paper we consider decision-fusion based on energy detection over Ricean-mixture fading channels. The system under investigation is made of a WSN reporting individual-sensor decisions about a binary source to a FC equipped with multiple antennas. Although the reporting phase from the sensors to the FC may have some analogies with a standard multiuser system, the following peculiarities differentiate the considered system from an usual communication system: (i) there are two sources of impairment (one at sensor location due to the sensing phase and the other at FC location due to the reporting phase), (ii) the final goal is the detection of the underlying state of the source, without special interest on the reconstruction at the FC of the local decision of each individual sensor. More specifically, we analyze the case in which hard decision is performed by each sensor and channel coefficients on sensors-to-FC links are modeled collectively as a vector Gaussian mixture (GM). GMs is a general model that can take into account multi-modality, asymmetry, heavy tails, and other characteristics that may be present in real-world scenarios, though exhibiting interesting properties in terms of mathematical tractability [19]. Recently, they have been proposed as a powerful tool for modeling arbitrary wireless fading channels and compared with classical composite models (e.g. Nakagami-Lognormal fading) capturing multipath fading and shadowing effects [20], [21]. Real-world channels exhibit parameter variability (due to spatial and/or temporal dynamics) which a GM model is able to incorporate. Furthermore, real-world measurements of fading distributions in WSNs have been recently matched to mixtures models, which are able to capture the statistics over long intervals and include significant changes in the environment, e.g. mixtures of Gamma distributions have been proposed in [22] to characterize the received signals in the power domain. Also, it is worth noticing that both Ricean and Rayleigh channels (widely used in the literature) are special cases of the general GM model considered here.

B. Contribution and Organization of the Paper

The paper builds upon the work in [23] which focused on the case where all the sensors have identical local performance (namely *homogeneous scenario*) and the FC is equipped with a single receiving antenna (thus using a scalar GM model). Here we assume consider both homogeneous and non-homogeneous scenarios, a FC with arbitrary number of receiving antennas (thus using a vectorial GM model) and provide a deeper analysis which includes comparison of the optimal and energy tests for large-system scenarios. Although we focus on a single-hop centralized architecture, the receiving approach at the FC can be apparently implemented at each intermediate node in a multi-hop architecture. Summarizing, the main contributions of this paper are:

- to the best of authors' knowledge, the use of a GM vector model is proposed for the first time in the framework of decision fusion with WSNs;
- the derivation of the optimal test, i.e. based on log-likelihood ratio (LLR), and the complete performance characterization (in terms of global probabilities of false alarm and detection) of a low-complexity sub-optimal test based on energy detection for the aforementioned GM model;
- performance analysis of large-size WSNs is obtained through the asymptotic analysis of both optimal and energy tests[1] assuming either an individual power constraint (IPC) on each single sensor (which is more interesting for systems using pre-defined sensors with given performance) or a total power constraint (TPC) on the whole set of sensors (which is more appealing when sensors could be designed in advance);
- all the results are derived for both homogenous (i.e. sensors with identical local performance) and non-homogeneous (i.e. non-identical sensors) scenarios;
- validation of the provided theoretical results through numerical simulations, which also demonstrate the flexibility of the proposed model;
- a final example illustrating how the presented results can be used for average performance evaluation of realistic complex scenarios with unknown sensor positions.

The outline of the paper is the following: Sec. II collects some useful results on GM random vectors which are exploited in the remainder of the paper; in Sec. III we present the system model under investigation; in Sec. IV we describe the statistics for the global decision at the FC, the figures for system-performance evaluation, the optimal and the energy tests, and the analytical performance for the latter; the asymptotic analysis for performance-evaluation of large-size WSNs is developed in Sec. V; theoretical results are validated through numerical results in Sec. VI which also highlights and compares the performance of simulated systems with different setups; some concluding remarks are given in Sec. VII.

C. Notation

Lower-case bold letters denote vectors, with a_n denoting the nth element of $\boldsymbol{a}$; upper-case bold letters denote matrices, with $A_{n,m}$ denoting the (n, m)th element of $\boldsymbol{A}$; $\boldsymbol{I}_N$ and $\boldsymbol{O}_N$ denote the $N \times N$ identity and null matrices, respectively; $\mathbf{0}_N$ and $\mathbf{1}_N$ denote the N-length column vectors whose elements are 0 and 1, respectively; $\text{diag}(\boldsymbol{a})$ denotes a diagonal matrix with $\boldsymbol{a}$ on the main diagonal; $(\cdot)^t$, $(\cdot)^*$, $(\cdot)^\dagger$, $\det(\boldsymbol{A})$, $\otimes$, $\mathbb{E}\{\cdot\}$, $\mathbb{C}\text{ov}\{\cdot\}$, $\text{p}\mathbb{C}\text{ov}\{\cdot\}$, $\|\cdot\|$, $\Re(\cdot)$, $\Im(\cdot)$, and $|\cdot|$ denote transpose, conjugate, conjugate transpose, determinant, Kronecker product, expectation, covariance, pseudocovariance, Euclidean norm, real part,

[1]The analysis is based on the use of multivariate versions of the central limit theorem (CLT) for complex-valued improper Gaussian random vectors.

imaginary part, and modulus operators, respectively; j is the imaginary unit; $\Pr(\mathcal{A})$ denotes the probability of the event $\mathcal{A}$; $p(a)$, $P(a)$ and $\phi_a(\cdot)$ denote the probability density function (PDF), the complementary cumulative distribution function (CCDF) and the characteristic function (CF), respectively, of the random variable (RV) a; $\mathcal{A}^n$ denotes the nth Cartesian power of the set $\mathcal{A}$; $\binom{\ell}{\boldsymbol{m}} = \frac{\ell!}{m_1!\ldots m_M!}$ is the multinomial coefficient; $\mathcal{N}_{\mathbb{C}}(\boldsymbol{\mu}; \boldsymbol{\Omega}, \boldsymbol{\Upsilon})$ denotes an improper complex-valued normal distribution with mean vector $\boldsymbol{\mu}$, covariance matrix $\boldsymbol{\Omega}$, and pseudocovariance matrix $\boldsymbol{\Upsilon}$; $\mathcal{N}_{\mathbb{C}}(\boldsymbol{\mu}; \boldsymbol{\Omega})$ will be used as a short notation for $\mathcal{N}_{\mathbb{C}}(\boldsymbol{\mu}; \boldsymbol{\Omega}, \boldsymbol{O}_N)$, i.e. a proper complex-valued normal distribution; a circularly-symmetric complex-valued Gaussian distribution will be denoted $\mathcal{N}_{\mathbb{C}}(\boldsymbol{0}_N; \boldsymbol{\Omega})$; $\chi^2_N(\alpha; \beta)$ denotes a scaled non-central chi-square distribution with N degrees of freedom, non-centrality parameter α and scale parameter $\sqrt{\beta}$; the symbols $\sim$ and $\overset{(a)}{\sim}$ mean "distributed as" and "asymptotically distributed as", respectively.

We recall the definitions of the modified Bessel function of the first kind, Q-function, generalized Marcum Q-function and upper incomplete Gamma function, respectively as

$$I_n(x) = \frac{1}{\pi}\int_0^{\pi} \exp\left(x\cos(\theta)\right)\cos(n\theta)d\theta, \tag{1}$$

$$Q(x) = \frac{1}{\sqrt{2\pi}}\int_x^{\infty} \exp\left(-\frac{\xi^2}{2}\right)d\xi, \tag{2}$$

$$Q_m(a; b) = \int_b^{\infty} \frac{\xi^m}{a^{m-1}} \exp\left(-\frac{\xi^2 + a^2}{2}\right) I_{m-1}\left(a\xi\right)d\xi, \tag{3}$$

$$\Gamma(a, b) = \int_b^{\infty} \xi^{a-1}\exp(-\xi)d\xi. \tag{4}$$

while the Gamma function is defined as $\Gamma(a) = \Gamma(a, 0)$.

II. Preliminaries on GM RVs

In this section we review some useful results on GM RVs [24]–[28], summarized in the following propositions and in the final theorem.

Proposition 1: Consider an $N-$dimensional vector $\boldsymbol{x}$ modeled as an M-component complex GM

$$\boldsymbol{x} \sim \sum_{m=1}^{M} \rho_m \mathcal{N}_{\mathbb{C}}\left(\boldsymbol{\mu}_m; \sigma_m^2 \boldsymbol{I}_N\right). \tag{5}$$

Using the total probability theorem, it is straightforward to show that the quadratic form $y = \|\boldsymbol{x}\|^2$ is a scaled non-central chi-square mixture, i.e. $y \sim \sum_{m=1}^{M} \rho_m \chi^2_{2N}(\|\mu_m\|^2; \sigma_m^2)$ with its PDF, CCDF and CF being

$$p(y) = \sum_{m=1}^{M} \frac{\rho_m}{\sigma_m^2}\left(\frac{y}{\|\boldsymbol{\mu}_m\|^2}\right)^{\frac{N-1}{2}} \exp\left(-\frac{y + \|\boldsymbol{\mu}_m\|^2}{\sigma_m^2}\right) \times I_{N-1}\left(\frac{2\|\boldsymbol{\mu}_m\|\sqrt{y}}{\sigma_m^2}\right) \tag{6}$$

$$P(y) = \sum_{m=1}^{M} \rho_m Q_N\left(\frac{\sqrt{2}\|\boldsymbol{\mu}_m\|}{\sigma_m}, \frac{\sqrt{2y}}{\sigma_m}\right), \tag{7}$$

$$\phi_y(\tau) = \sum_{m=1}^{M} \frac{\rho_m}{\left(1 - j\tau\sigma_m^2\right)^N} \exp\left(\frac{j\tau\|\boldsymbol{\mu}_m\|^2}{1 - j\tau\sigma_m^2}\right). \tag{8}$$

Such a result will be exploited in Sec. IV-B for performance evaluation of the received-energy test.

Proposition 2: Consider a set of $N-$dimensional independent and identically-distributed (IID) vectors $\{\boldsymbol{x}_1, \ldots, \boldsymbol{x}_K\}$ each being modeled as an M-component complex GM, i.e. as in (5), and a set of coefficients $\{c_1, \ldots, c_K\}$, then the linear combination $\boldsymbol{y} = \sum_{k=1}^{K} c_k \boldsymbol{x}_k$ is a complex GM with $\binom{M+K-1}{K}$ components, i.e.

$$\boldsymbol{y} \sim \sum_{m_1=1}^{M} \cdots \sum_{m_K=1}^{M} \rho_{m_1} \cdots \rho_{m_K} \mathcal{N}_{\mathbb{C}}\left(\boldsymbol{\nu}_{m_1,\ldots,m_K}; \omega^2_{m_1,\ldots,m_K} \boldsymbol{I}_N\right), \tag{9}$$

where the mean vector and the variance of the generic component of the resulting GM are $\boldsymbol{\nu}_{m_1,\ldots,m_K} = \sum_{k=1}^{K} c_k \boldsymbol{\mu}_{m_k}$ and $\omega^2_{m_1,\ldots,m_K} = \sum_{k=1}^{K} |c_k|^2 \sigma^2_{m_k}$. Such a result will be exploited in Sec. IV-A for statistical characterization of the signal received at FC.

Proposition 3: Consider a set of $N-$dimensional IID complex-valued vectors $\{\boldsymbol{x}_1, \ldots, \boldsymbol{x}_K\}$ sampled from an arbitrary distribution with mean vector $\boldsymbol{\mu}$ and finite positive definite covariance and pseudocovariance matrices $\boldsymbol{\Omega}$ and $\boldsymbol{\Upsilon}$, and define the sample mean vector as $\bar{\boldsymbol{x}} = \frac{1}{K}\sum_{k=1}^{K} \boldsymbol{x}_k$, then

$$\sqrt{K}(\bar{\boldsymbol{x}} - \boldsymbol{\mu}) \overset{(a)}{\sim} \mathcal{N}_{\mathbb{C}}(\boldsymbol{0}_N, \boldsymbol{\Omega}, \boldsymbol{\Upsilon}), \tag{10}$$

This result is known as Lindeberg-Levy multivariate CLT (see [25] for the real-valued case).

Proposition 4: Consider a set of $N-$dimensional independent and non-identically-distributed (INID) complex-valued vectors $\{\boldsymbol{x}_1, \ldots, \boldsymbol{x}_K\}$ sampled from a set of arbitrary distributions with corresponding mean vectors $\{\boldsymbol{\mu}_1, \ldots, \boldsymbol{\mu}_K\}$ and finite positive definite covariance and pseudocovariances matrices $\{\boldsymbol{\Omega}_1, \ldots, \boldsymbol{\Omega}_K\}$ and $\{\boldsymbol{\Upsilon}_1, \ldots, \boldsymbol{\Upsilon}_K\}$, respectively. Define $\bar{\boldsymbol{\mu}}_K = \frac{1}{K}\sum_{k=1}^{K} \boldsymbol{\mu}_k$, $\bar{\boldsymbol{\Omega}}_K = \frac{1}{K}\sum_{k=1}^{K} \boldsymbol{\Omega}_k$, and $\bar{\boldsymbol{\Upsilon}}_K = \frac{1}{K}\sum_{k=1}^{K} \boldsymbol{\Upsilon}_k$. Assume that all mixed third-order moments are finite and that

$$\lim_{K\to\infty} \boldsymbol{\Omega}_K = \boldsymbol{\Omega}, \quad \lim_{K\to\infty} \boldsymbol{\Upsilon}_K = \boldsymbol{\Upsilon}, \tag{11}$$

$$\lim_{K\to\infty} \left(K\bar{\boldsymbol{\Omega}}_K\right)^{-1} \boldsymbol{\Omega}_k = \boldsymbol{O}_N, \quad \lim_{K\to\infty} \left(K\bar{\boldsymbol{\Upsilon}}_K\right)^{-1} \boldsymbol{\Upsilon}_k = \boldsymbol{O}_N, \tag{12}$$

then

$$\sqrt{K}(\bar{\boldsymbol{x}} - \boldsymbol{\mu}) \overset{(a)}{\sim} \mathcal{N}_{\mathbb{C}}(\boldsymbol{0}_N, \boldsymbol{\Omega}, \boldsymbol{\Upsilon}), \tag{13}$$

Such a generalization is known as Lindeberg-Feller multivariate CLT (see [25] for the real-valued case).

Proposition 5: Consider a proper complex-valued N-length Gaussian random vector $\boldsymbol{x}$ with arbitrary mean vector and covariance matrix, i.e. $\boldsymbol{x} \sim \mathcal{N}_{\mathbb{C}}(\boldsymbol{\mu}; \boldsymbol{\Omega})$, then the CF of the quadratic form $y = \boldsymbol{x}^{\dagger}\boldsymbol{A}\boldsymbol{x}$, with $\boldsymbol{A}$ being an arbitrary Hermitian matrix, is (see [26] for details)

$$\phi_y(\tau) = \frac{\exp\left(-\boldsymbol{\mu}^{\dagger}\boldsymbol{\Omega}^{-1}\left(\boldsymbol{I}_N - (\boldsymbol{I}_N - j\tau\boldsymbol{\Omega}\boldsymbol{A})^{-1}\right)\boldsymbol{\mu}\right)}{\det(\boldsymbol{I}_N - j\tau\boldsymbol{\Omega}\boldsymbol{A})}. \tag{14}$$

Expanding the previous results, we get the following

Theorem 1: Consider an improper complex-valued N-length Gaussian random vector $\boldsymbol{x}$ with arbitrary mean vector, covariance and pseudocovariance matrices,

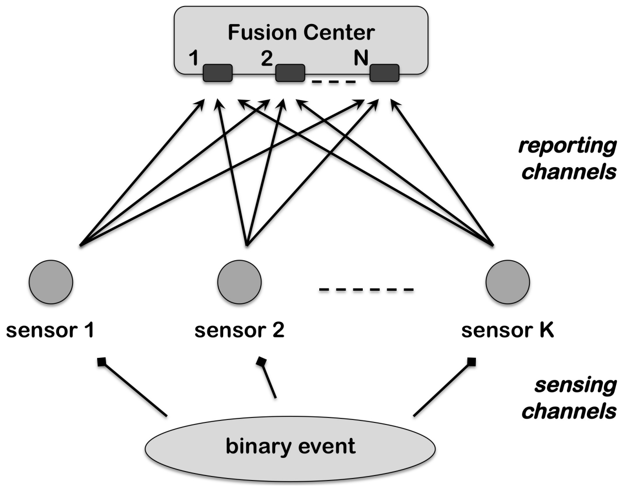

Fig. 1. Scenario for collaborative binary decision through a WSN with K sensors and one FC equipped with N antennas.

i.e. $\boldsymbol{x} \sim \mathcal{N}_{\mathbb{C}}(\boldsymbol{\mu}; \boldsymbol{\Omega}, \boldsymbol{\Upsilon})$, and the corresponding augmented representation [28], i.e.

$$\underline{\boldsymbol{x}} = \left(\boldsymbol{x}^t, \boldsymbol{x}^\dagger\right)^t, \quad \underline{\boldsymbol{\mu}} = \left(\boldsymbol{\mu}^t, \boldsymbol{\mu}^\dagger\right)^t, \quad \underline{\boldsymbol{\Omega}} = \begin{pmatrix} \boldsymbol{\Omega} & \boldsymbol{\Upsilon} \\ \boldsymbol{\Upsilon}^* & \boldsymbol{\Omega}^* \end{pmatrix}, \quad (15)$$

then the CF of the augmented quadratic form $y = \frac{1}{2}\underline{\boldsymbol{x}}^\dagger \underline{\boldsymbol{A}} \underline{\boldsymbol{x}} = \boldsymbol{x}^\dagger \boldsymbol{E} \boldsymbol{x} + \Re\left\{\boldsymbol{x}^\dagger \boldsymbol{F} \boldsymbol{x}^*\right\}$, with $\underline{\boldsymbol{A}}$ being an augmented Hermitian matrix, i.e. having the following structure

$$\underline{\boldsymbol{A}} = \begin{pmatrix} \boldsymbol{E} & \boldsymbol{F} \\ \boldsymbol{F}^* & \boldsymbol{E}^* \end{pmatrix}, \quad \boldsymbol{E}^\dagger = \boldsymbol{E}, \ \boldsymbol{F}^t = \boldsymbol{F}, \quad (16)$$

is (see Appendix A for the proof)

$$\phi_y(\tau) = \frac{\exp\left(-\frac{1}{2}\underline{\boldsymbol{\mu}}^\dagger \underline{\boldsymbol{\Omega}}^{-1}\left(\boldsymbol{I}_{2N} - (\boldsymbol{I}_{2N} - j\tau\underline{\boldsymbol{\Omega}}\ \underline{\boldsymbol{A}})^{-1}\right)\underline{\boldsymbol{\mu}}\right)}{\det^{1/2}(\boldsymbol{I}_{2N} - j\tau\underline{\boldsymbol{\Omega}}\ \underline{\boldsymbol{A}})}. \quad (17)$$

It is worth noticing that (17) generalizes (14).

III. System Model

As shown in Fig. 1, we consider a scenario in which K sensors sense a binary phenomenon of interest, each taking autonomously a local decision. The two hypotheses are denoted $\mathcal{H}_0$ and $\mathcal{H}_1$ and the corresponding a-priori probabilities π_0 and π_1, respectively. We assume that the local sensing and decision process at the kth sensor is fully described by the local probability of false alarm ($p_{f,k}$) and the local probability of detection ($p_{d,k}$), with local decision being conditionally independent given the specific hypothesis. In the case of homogeneous scenarios, local probabilities of false alarm and detection will be denoted p_f and p_d, respectively. Sensors, each with one single transmit antenna, communicate simultaneously their decision to a FC, equipped with N receive antennas, whose aim is to provide a robust decision on the basis of the multiple received information. All the sensors employ the same binary modulation, for energy saving purposes we consider OOK modulation, with identical parameters (transmission pulse, carrier frequency, etc.). We assume that the system is fully synchronized: the impact of synchronization errors on system performance falls beyond the scope of this paper.

A. Signal Model

We denote: $x_k \in \mathcal{X} = \{0, 1\}$ the symbol transmitted by the kth sensor encoding its local decision (we assume $x_k = i$ for $\mathcal{H}_i$); $H_{n,k}$ the fading channel coefficient on the link between the kth sensor and the nth receive antenna; y_n the signal received by the nth antenna at the FC; and w_n the additive white Gaussian noise at the nth receive antenna. We denote $\boldsymbol{h}_{(k)} = \left(H_{1,k}, \ldots, H_{N,k}\right)^t$ the kth channel vector, collecting the fading coefficients on the links from the kth sensor to all the antennas at the FC.

The discrete-time model for the received signal is

$$\boldsymbol{y} = \sum_{k=1}^{K} \boldsymbol{h}_{(k)} x_k + \boldsymbol{w} = \boldsymbol{H}\boldsymbol{x} + \boldsymbol{w}. \quad (18)$$

where $\boldsymbol{y} = (y_1, \ldots, y_N)^t$ is the received signal vector, $\boldsymbol{w} = (w_1, \ldots, w_N)^t \sim \mathcal{N}_{\mathbb{C}}(\boldsymbol{0}_N; \sigma_w^2 \boldsymbol{I}_N)$ is the noise contribution, $\boldsymbol{H} = \left(\boldsymbol{h}_{(1)}, \ldots, \boldsymbol{h}_{(K)}\right)$ is the channel matrix, and $\boldsymbol{x} = (x_1, \ldots, x_K)^t$ is the transmitted vector (of local decisions).

B. Channel Model

Channel vectors are assumed IID $N-$dimensional complex GM with M components, i.e.

$$\boldsymbol{h}_{(k)} \sim \sum_{m=1}^{M} \rho_m \mathcal{N}_{\mathbb{C}}\left(\boldsymbol{\mu}_m; \sigma_m^2 \boldsymbol{I}_N\right), \quad (19)$$

where $\boldsymbol{\mu}_m = \left(\mu_{m,1}, \ldots, \mu_{m,N}\right)^t$ and $\sigma_m^2 \boldsymbol{I}_N$ represent the mean vector and the covariance matrix of the mth component of the GM, respectively. Also, we collect the parameters of the GM by defining $\boldsymbol{\rho} = (\rho_1, \ldots, \rho_M)^t$, and (with a slight abuse of notation) $\boldsymbol{\sigma}^2 = \left(\sigma_1^2, \ldots, \sigma_M^2\right)^t$. The general GM model, with different components having different mean vectors (or steering vectors), allows for simulation of a set of sensors with arbitrary angular distribution, i.e. a WSN with location-dependent spatial diversity, as investigated in the numerical analysis of Sec. VI.

Although the IID assumption may appear unrealistic at first, Section VI-B clarifies how the proposed work is able to capture the average performance of system in realistic scenarios with channel distribution depending on the specific location of the sensors. The reason is that the system performance depends on the ensemble distribution at the FC (given by the superposition of the received signals from all the sensors) which is well modeled as a GM.

In order to further emphasize the interest towards the GM model, we stress that it represents the proper approach to handle scenarios in which the location of the sensors is unknown, but a statistical information in terms of location probability distribution may be assumed [29], [30]. More specifically, the channel from the kth sensor could be fairly assumed to be Rician with parameters depending on the location ($\boldsymbol{u}_k$) of the sensor itself, i.e. $\boldsymbol{h}_{(k)} \sim \mathcal{N}_{\mathbb{C}}\left(\boldsymbol{\mu}_k(\boldsymbol{u}_k); \sigma_k^2(\boldsymbol{u}_k)\boldsymbol{I}_N\right)$. If the location probability distribution of the sensors ($p(\boldsymbol{u}_k)$) is available, it might be exploited through marginalization, i.e.

$$\boldsymbol{h}_{(k)} \sim \int p(\boldsymbol{u}_k) \mathcal{N}_{\mathbb{C}}\left(\boldsymbol{\mu}_k(\boldsymbol{u}_k); \sigma_k^2(\boldsymbol{u}_k)\boldsymbol{I}_N\right) d\boldsymbol{u}_k. \quad (20)$$

Unfortunately, such a task is typically intractable, and approximations based on Riemann sums must be considered. More specifically, the location domain is partitioned into a finite number of regions ($\{\mathcal{S}_m\}_{m=1}^M$) each represented by a corresponding sample position ($\{\boldsymbol{u}_k[m]\}_{m=1}^M$). Then (20) is approximated as

$$\boldsymbol{h}_{(k)} \sim \sum_{m=1}^{M} \Pr(\boldsymbol{u}_k \in \mathcal{S}_m)\mathcal{N}_{\mathbb{C}}\left(\boldsymbol{\mu}_k(\boldsymbol{u}_k[m]); \sigma_k^2(\boldsymbol{u}_k[m])\boldsymbol{I}_N\right), \tag{21}$$

which fits the GM model in (19) by denoting $\rho_m = \Pr(\boldsymbol{u}_k \in \mathcal{S}_m)$, $\boldsymbol{\mu}_m = \boldsymbol{\mu}_k(\boldsymbol{u}_k[m])$, and $\sigma_m^2 = \sigma_k^2(\boldsymbol{u}_k[m])$.

Given the statistical characterization in (19), it is not difficult to show that the first- and second-order moments of the channel vectors $\boldsymbol{h}_{(k)}$ are

$$\boldsymbol{\mu}_H = \mathbb{E}\left\{\boldsymbol{h}_{(k)}\right\} = \sum_{m=1}^{M} \rho_m \boldsymbol{\mu}_m, \tag{22}$$

$$\boldsymbol{R}_H = \mathbb{E}\left\{\boldsymbol{h}_{(k)}\boldsymbol{h}_{(k)}^{\dagger}\right\} = \sum_{m=1}^{M} \rho_m(\sigma_m^2\boldsymbol{I}_N + \boldsymbol{\mu}_m\boldsymbol{\mu}_m^{\dagger}), \tag{23}$$

$$\boldsymbol{Q}_H = \mathbb{E}\left\{\boldsymbol{h}_{(k)}\boldsymbol{h}_{(k)}^{t}\right\} = \sum_{m=1}^{M} \rho_m \boldsymbol{\mu}_m\boldsymbol{\mu}_m^{t}. \tag{24}$$

The analysis for the decision fusion is made for a general GM channel model whereas specific results are reported for *three special cases*:

- one single nonzero-mean component, namely *Rice fading*;
- two zero-mean components, here called *2ZM fading*;
- one nonzero-mean and one zero-mean components, here called *NZZ fading*.

The first two cases represent the simplest extensions for the case with one single zero-mean component, i.e. *Rayleigh fading*, analyzed in [15]. The latter case is a combination of the first two. More specifically, in Rice fading

$$\boldsymbol{h}_{(k)} \sim \mathcal{N}_{\mathbb{C}}\left(\boldsymbol{\mu}_1; \sigma_1^2\boldsymbol{I}_N\right), \tag{25}$$

while in 2ZM fading

$$\boldsymbol{h}_{(k)} \sim \rho_1\mathcal{N}_{\mathbb{C}}\left(\boldsymbol{0}_N; \sigma_1^2\boldsymbol{I}_N\right) + \rho_2\mathcal{N}_{\mathbb{C}}\left(\boldsymbol{0}_N; \sigma_2^2\boldsymbol{I}_N\right), \tag{26}$$

and in NZZ fading

$$\boldsymbol{h}_{(k)} \sim \rho_1\mathcal{N}_{\mathbb{C}}\left(\boldsymbol{\mu}_1; \sigma_1^2\boldsymbol{I}_N\right) + \rho_2\mathcal{N}_{\mathbb{C}}\left(\boldsymbol{0}_N; \sigma_2^2\boldsymbol{I}_N\right). \tag{27}$$

Although unrealistic from a practical point of view, assuming a Rice fading model with same mean vector (or steering vector) for each sensor is still interesting because it introduces the effect of a non-zero mean while keeping simple the mathematical details. Tab. I shows explicitly the first- and second-order moments of $\boldsymbol{h}_{(k)}$ for Rice, 2ZM and NZZ fading.

IV. Decision Fusion

The decision is usually performed as a test comparing a signal-dependent statistic ($\lambda(\boldsymbol{y})$) and a fixed threshold (γ)

$$\lambda(\boldsymbol{y}) \underset{\hat{\mathcal{H}}=\mathcal{H}_0}{\overset{\hat{\mathcal{H}}=\mathcal{H}_1}{\gtrless}} \gamma, \tag{28}$$

TABLE I

First- and Second-Order Moments of $\boldsymbol{h}_{(k)}$

	$\boldsymbol{\mu}_H$	$\boldsymbol{R}_H$	$\boldsymbol{Q}_H$
Rice	$\boldsymbol{\mu}_1$	$\sigma_1^2\boldsymbol{I}_N + \boldsymbol{\mu}_1\boldsymbol{\mu}_1^{\dagger}$	$\boldsymbol{\mu}_1\boldsymbol{\mu}_1^{t}$
2ZM	$\boldsymbol{0}_N$	$(\rho_1\sigma_1^2 + \rho_2\sigma_2^2)\boldsymbol{I}_N$	$\boldsymbol{O}_N$
NZZ	$\rho_1\boldsymbol{\mu}_1$	$(\rho_1\sigma_1^2 + \rho_2\sigma_2^2)\boldsymbol{I}_N + \rho_1\boldsymbol{\mu}_1\boldsymbol{\mu}_1^{\dagger}$	$\rho_1\boldsymbol{\mu}_1\boldsymbol{\mu}_1^{t}$

where $\hat{\mathcal{H}}$ denotes the declared hypothesis. Performance is evaluated in terms of global probability of false alarm (q_f) and global probability of detection (q_d), defined as follows

$$q_f = \Pr\left(\lambda > \gamma\,|\mathcal{H}_0\right), \quad q_d = \Pr\left(\lambda > \gamma\,|\mathcal{H}_1\right). \tag{29}$$

It is worth noticing that $\Pr(\lambda > \gamma\,|\mathcal{H}_i)$ generically describes both q_f and q_d (with $i = 0$ and $i = 1$, respectively). The behavior of the global probability of detection (q_d) versus the global probability of false alarm (q_f) is commonly denoted *receiver operating characteristic* (ROC). The threshold in (28) is usually selected in order to keep a fixed probability of false alarm (according to the Neyman-Pearson criterion) or minimize the fusion error probability $q_e = \pi_0 q_f + \pi_1(1 - q_d)$ (according to the Bayes criterion) [31].

A. Optimal Test

The LLR of the received signal under the two hypotheses provides the optimal test [31]

$$\lambda(\boldsymbol{y}) = \log\left(\frac{p(\boldsymbol{y}|\mathcal{H}_1)}{p(\boldsymbol{y}|\mathcal{H}_0)}\right) = \log\left(\frac{\sum_{\ell=0}^{K} p(\boldsymbol{y}|\ell)\Pr(\ell|\mathcal{H}_1)}{\sum_{\ell=0}^{K} p(\boldsymbol{y}|\ell)\Pr(\ell|\mathcal{H}_0)}\right), \tag{30}$$

where $\ell = \boldsymbol{x}^t\boldsymbol{1}_K$ is the number of sensors transmitting 1. Eq. (30) is explained by noticing that: sensor decisions are conditionally independent; OOK is the modulation format; channel vectors are IID. From Prop. (2), it is straightforward to show that

$$p(\boldsymbol{y}|\ell) = \sum_{\boldsymbol{m}^t\boldsymbol{1}_M=\ell} \frac{\theta_{\boldsymbol{m}}(\ell)}{(\pi\omega_{\boldsymbol{m}}^2)^N}\exp\left(-\frac{\|\boldsymbol{y} - \boldsymbol{v}_{\boldsymbol{m}}\|^2}{\omega_{\boldsymbol{m}}^2}\right), \tag{31}$$

where $\boldsymbol{m} = (m_1, \ldots, m_M)^t$ is a vector of integers (with m_u representing the number of links experiencing the uth component of the complex GM) denoting the aggregate component of the new resulting GM, $\theta_{\boldsymbol{m}}(\ell) = \binom{\ell}{\boldsymbol{m}}\exp(\boldsymbol{m}^t\log(\boldsymbol{\rho}))$ is the probability of the aggregate component, $\boldsymbol{v}_{\boldsymbol{m}} = \sum_{u=1}^{M} m_u\boldsymbol{\mu}_u$ is the mean vector of the aggregate component, and $\omega_{\boldsymbol{m}}^2 = \boldsymbol{m}^t\boldsymbol{\sigma}^2 + \sigma_w^2$ is the variance of the aggregate component. Eq. (31) clearly shows that the conditional signal at each receive antenna is a GM with $L(\ell) = \binom{M+\ell-1}{\ell}$ components, denoted hereinafter, for sake of simplicity, as

$$\boldsymbol{y}|\ell \sim \sum_{m=1}^{L(\ell)} \theta_m(\ell)\mathcal{N}_{\mathbb{C}}\left(\boldsymbol{v}_m(\ell); \omega_m^2(\ell)\boldsymbol{I}_N\right). \tag{32}$$

More specifically, in Rice fading

$$p(\boldsymbol{y}|\ell) = \frac{1}{\pi^N\left(\ell\sigma_1^2 + \sigma_w^2\right)^N}\exp\left(-\frac{\|\boldsymbol{y} - \ell\boldsymbol{\mu}_1\|^2}{\ell\sigma_1^2 + \sigma_w^2}\right), \tag{33}$$

while in 2ZM fading

$$p(\boldsymbol{y}|\ell) = \sum_{m=0}^{\ell} \binom{\ell}{m} \frac{(\rho_1)^m (\rho_2)^{\ell-m}}{\pi^N \left(m\sigma_1^2 + (\ell-m)\sigma_2^2 + \sigma_w^2\right)^N} \times \exp\left(-\frac{\|\boldsymbol{y}\|^2}{m\sigma_1^2 + (\ell-m)\sigma_2^2 + \sigma_w^2}\right), \quad (34)$$

and in NZZ fading

$$p(\boldsymbol{y}|\ell) = \sum_{m=0}^{\ell} \binom{\ell}{m} \frac{(\rho_1)^m (\rho_2)^{\ell-m}}{\pi^N \left(m\sigma_1^2 + (\ell-m)\sigma_2^2 + \sigma_w^2\right)^N} \times \exp\left(-\frac{\|\boldsymbol{y} - m\boldsymbol{\mu}_1\|^2}{m\sigma_1^2 + (\ell-m)\sigma_2^2 + \sigma_w^2}\right). \quad (35)$$

Furthermore, it is worth noticing that in the case of homogeneous scenarios, $\ell|\mathcal{H}_i$ is a binomial RV, i.e.

$$\Pr(\ell|\mathcal{H}_i) = \binom{K}{\ell} p_i^{\ell} (1-p_i)^{K-\ell}, \quad (36)$$

where $p_i = p_f$ (resp. $p_i = p_d$) in the case $\mathcal{H}_0$ (resp. $\mathcal{H}_1$), while in the case of non-homogeneous scenarios, $\ell|\mathcal{H}_i$ is a Poisson-binomial RV, i.e.

$$\Pr(\ell|\mathcal{H}_i) = \sum_{\boldsymbol{x}:\boldsymbol{x}^t\boldsymbol{1}_K=\ell} \left(\prod_{k=1}^{K} p_{i,k}^{x_k}\right)\left(\prod_{k=1}^{K} (1-p_{i,k})^{1-x_k}\right), \quad (37)$$

where $p_{i,k} = p_{f,k}$ (resp. $p_{i,k} = p_{d,k}$) under $\mathcal{H}_0$ (resp. $\mathcal{H}_1$). Various techniques (e.g. refer to [32]) have been proposed for efficient evaluation of (37).

However, the optimal test is computationally expensive and additionally has high knowledge requirements (statistical CSI, SNR level and local sensor performance).

B. Energy Test and Performance Analysis

In the case of OOK, a common simpler alternative is obtained replacing the LLR with the energy of the received signal, i.e.

$$\lambda(\boldsymbol{y}) = \|\boldsymbol{y}\|^2, \quad (38)$$

which apparently requires little computational complexity and also has the advantage that neither CSI nor SNR nor local sensor performance are needed. Such a test has been proved to be optimal in Rayleigh fading scenarios [9], [15] and near-optimal in *non-line-of-sight* fading scenarios [16].

The conditional statistic $\lambda|\ell$ is the energy of the GM-distributed random vector in (32), then, the CCDF of $\lambda|\ell$ has an analogous expression to the right term in (7) when replacing M, ρ_m, $\boldsymbol{\mu}_m$ and σ_m^2, with $L(\ell)$, $\theta_m(\ell)$, $\boldsymbol{v}_m(\ell)$ and $\omega_m^2(\ell)$, respectively. Using the total probability theorem and combining Prop. 1 with (29), we get

$$\Pr(\lambda > \gamma|\mathcal{H}_i) = \sum_{\ell=0}^{K} \sum_{m=1}^{L(\ell)} \Pr(\ell|\mathcal{H}_i)\theta_m(\ell) \times Q_N\left(\frac{\sqrt{2}\|\boldsymbol{v}_m(\ell)\|}{\omega_m(\ell)}, \frac{\sqrt{2\gamma}}{\omega_m(\ell)}\right). \quad (39)$$

More specifically, in Rice fading, 2ZM fading and NZZ fading we obtain Eqs. (40), (41) and (42) at the bottom of this page, respectively.

V. Asymptotic Analysis

It can be shown (see Appendix B) that the first- and central second-order moments of $\boldsymbol{y}|\mathcal{H}_i$ are

$$\mathbb{E}\{\boldsymbol{y}|\mathcal{H}_i\} = S_{p_i}\boldsymbol{\mu}_H, \quad (43)$$

$$\mathbb{C}\mathrm{ov}\{\boldsymbol{y}|\mathcal{H}_i\} = S_{p_i}\boldsymbol{R}_H - S_{p_i^2}\boldsymbol{\mu}_H\boldsymbol{\mu}_H^{\dagger} + \sigma_w^2\boldsymbol{I}_N, \quad (44)$$

$$\mathrm{p}\mathbb{C}\mathrm{ov}\{\boldsymbol{y}|\mathcal{H}_i\} = S_{p_i}\boldsymbol{Q}_H - S_{p_i^2}\boldsymbol{\mu}_H\boldsymbol{\mu}_H^{t}, \quad (45)$$

in the case of non-homogeneous scenarios, where we denoted

$$S_{p_i} = \left(\sum_{k=1}^{K} p_{i,k}\right), \quad S_{p_i^2} = \left(\sum_{k=1}^{K} p_{i,k}^2\right), \quad (46)$$

while in the case of homogeneous scenarios they become

$$\mathbb{E}\{\boldsymbol{y}|\mathcal{H}_i\} = Kp_i\boldsymbol{\mu}_H, \quad (47)$$

$$\mathbb{C}\mathrm{ov}\{\boldsymbol{y}|\mathcal{H}_i\} = Kp_i\left(\boldsymbol{R}_H - p_i\boldsymbol{\mu}_H\boldsymbol{\mu}_H^{\dagger}\right) + \sigma_w^2\boldsymbol{I}_N, \quad (48)$$

$$\mathrm{p}\mathbb{C}\mathrm{ov}\{\boldsymbol{y}|\mathcal{H}_i\} = Kp_i\left(\boldsymbol{Q}_H - p_i\boldsymbol{\mu}_H\boldsymbol{\mu}_H^{t}\right), \quad (49)$$

being $S_{p_i} = Kp_i$ and $S_{p_i^2} = Kp_i^2$.

If we consider a large-size (i.e. $K \gg 1$) WSN, we can use Props. 3 and 4 in order to characterize the received signal for homogenous and non-homogeneous scenarios, respectively. More specifically, if we assume that the WSN is made of sensors each subject to an IPC, we may apply the CLT to $\tilde{\boldsymbol{y}} \triangleq \boldsymbol{y}/\sqrt{K}$ and get

$$\tilde{\boldsymbol{y}}|\mathcal{H}_i - \tilde{\boldsymbol{\mu}}_i \overset{(a)}{\sim} \mathcal{N}_{\mathbb{C}}(\boldsymbol{0}_N; \boldsymbol{\Omega}_i, \boldsymbol{\Upsilon}_i), \quad (50)$$

$$\Pr(\lambda > \gamma|\mathcal{H}_i) = \sum_{\ell=0}^{K} \Pr(\ell|\mathcal{H}_i) Q_N\left(\frac{\sqrt{2}\ell\|\boldsymbol{\mu}_1\|}{\sqrt{\ell\sigma_1^2 + \sigma_w^2}}, \sqrt{\frac{2\gamma}{\ell\sigma_1^2 + \sigma_w^2}}\right), \quad (40)$$

$$\Pr(\lambda > \gamma|\mathcal{H}_i) = \sum_{\ell=0}^{K} \sum_{m=0}^{\ell} \Pr(\ell|\mathcal{H}_i) \binom{\ell}{m} \frac{\rho_1^m \rho_2^{\ell-m}}{\Gamma(N)} \Gamma\left(N, \frac{\gamma}{m\sigma_1^2 + (\ell-m)\sigma_2^2 + \sigma_w^2}\right), \quad (41)$$

$$\Pr(\lambda > \gamma|\mathcal{H}_i) = \sum_{\ell=0}^{K} \sum_{m=0}^{\ell} \Pr(\ell|\mathcal{H}_i) \binom{\ell}{m} \rho_1^m \rho_2^{\ell-m} Q_N\left(\frac{\sqrt{2}m\|\boldsymbol{\mu}_1\|}{\sqrt{m\sigma_1^2 + (\ell-m)\sigma_2^2 + \sigma_w^2}}, \sqrt{\frac{2\gamma}{m\sigma_1^2 + (\ell-m)\sigma_2^2 + \sigma_w^2}}\right). \quad (42)$$

TABLE II
ASYMPTOTIC MOMENTS OF THE CONDITIONAL RECEIVED SIGNAL FOR A WSN WITH IPC/TPC IN HOMOGENEOUS SCENARIOS

	$\tilde{\boldsymbol{\mu}}_i$ (IPC/TPC)	$\boldsymbol{\Omega}_i$ (IPC)	$\boldsymbol{\Omega}_i$ (TPC)	$\boldsymbol{\Upsilon}_i$ (IPC/TPC)
Rice	$\sqrt{K}p_i\boldsymbol{\mu}_1$	$p_i\sigma_1^2\boldsymbol{I}_N + p_i(1-p_i)\boldsymbol{\mu}_1\boldsymbol{\mu}_1^\dagger$	$(p_i\sigma_1^2+\sigma_w^2)\boldsymbol{I}_N + p_i(1-p_i)\boldsymbol{\mu}_1\boldsymbol{\mu}_1^\dagger$	$p_i(1-p_i)\boldsymbol{\mu}_1\boldsymbol{\mu}_1^t$
2ZM	$\boldsymbol{0}_N$	$p_i(\rho_1\sigma_1^2+\rho_2\sigma_2^2)\boldsymbol{I}_N$	$(p_i(\rho_1\sigma_1^2+\rho_2\sigma_2^2)+\sigma_w^2)\boldsymbol{I}_N$	$\boldsymbol{O}_N$
NZZ	$\sqrt{K}p_i\rho_1\boldsymbol{\mu}_1$	$p_i(\rho_1\sigma_1^2+\rho_2\sigma_2^2)\boldsymbol{I}_N + p_i\rho_1(1-p_i\rho_1)\boldsymbol{\mu}_1\boldsymbol{\mu}_1^\dagger$	$(p_i(\rho_1\sigma_1^2+\rho_2\sigma_2^2)+\sigma_w^2)\boldsymbol{I}_N + p_i\rho_1(1-p_i\rho_1)\boldsymbol{\mu}_1\boldsymbol{\mu}_1^\dagger$	$p_i\rho_1(1-p_i\rho_1)\boldsymbol{\mu}_1\boldsymbol{\mu}_1^t$

where in the case of non-homogeneous scenarios, from Eqs. (43), (44) and (45),

$$\tilde{\boldsymbol{\mu}}_i = \frac{S_{p_i}}{\sqrt{K}}\boldsymbol{\mu}_H, \tag{51}$$

$$\boldsymbol{\Omega}_i = \lim_{k\to\infty}\left(\frac{S_{p_i}}{K}\boldsymbol{R}_H - \frac{S_{p_i^2}}{K}\boldsymbol{\mu}_H\boldsymbol{\mu}_H^\dagger\right), \tag{52}$$

$$\boldsymbol{\Upsilon}_i = \lim_{k\to\infty}\left(\frac{S_{p_i}}{K}\boldsymbol{Q}_H - \frac{S_{p_i^2}}{K}\boldsymbol{\mu}_H\boldsymbol{\mu}_H^t\right). \tag{53}$$

while in the case of homogeneous scenarios, from Eqs. (47), (48) and (49),

$$\tilde{\boldsymbol{\mu}}_i = \sqrt{K}\,p_i\boldsymbol{\mu}_H, \tag{54}$$

$$\boldsymbol{\Omega}_i = p_i\left(\boldsymbol{R}_H - p_i\boldsymbol{\mu}_H\boldsymbol{\mu}_H^\dagger\right), \tag{55}$$

$$\boldsymbol{\Upsilon}_i = p_i\left(\boldsymbol{Q}_H - p_i\boldsymbol{\mu}_H\boldsymbol{\mu}_H^t\right). \tag{56}$$

Alternatively, if we assume that the whole WSN is subject to a TPC, we may apply the CLT to $\tilde{\boldsymbol{y}} \triangleq \boldsymbol{H}\boldsymbol{x}/\sqrt{K} + \boldsymbol{w}$ and get identical results for $\tilde{\boldsymbol{\mu}}_i$ and $\boldsymbol{\Upsilon}_i$, while $\boldsymbol{\Omega}_i$ is replaced with $\boldsymbol{\Omega}_i = \lim_{k\to\infty}\left(\frac{S_{p_i}}{K}\boldsymbol{R}_H - \frac{S_{p_i^2}}{K}\boldsymbol{\mu}_H\boldsymbol{\mu}_H^\dagger\right) + \sigma_w^2\boldsymbol{I}_N$ in the case of non-homogeneous scenarios and with $\boldsymbol{\Omega}_i = p_i\left(\boldsymbol{R}_H - p_i\boldsymbol{\mu}_H\boldsymbol{\mu}_H^\dagger\right) + \sigma_w^2\boldsymbol{I}_N$ in the case of homogeneous scenarios. More specifically, Tab. II shows explicitly the asymptotic moments of the received signal in the case of a WSN with IPC/TPC in homogeneous scenarios for Rice, 2ZM and NZZ fading.

Remark: Although the original model is based on a GM of proper Gaussian RV, it must be noticed that the limit distribution is an improper Gaussian.

Therefore, in order to deal effectively with an improper complex-valued Gaussian RV, we define the following augmented vectors and matrices [28]

$$\boldsymbol{y} = \left(\tilde{\boldsymbol{y}}^t, \tilde{\boldsymbol{y}}^\dagger\right)^t, \tag{57}$$

$$\boldsymbol{\mu}_i = \left(\mathbb{E}\{\tilde{\boldsymbol{y}}|\mathcal{H}_i\}^t, \mathbb{E}\{\tilde{\boldsymbol{y}}|\mathcal{H}_i\}^\dagger\right)^t = \left(\tilde{\boldsymbol{\mu}}_i^t, \tilde{\boldsymbol{\mu}}_i^\dagger\right)^t, \tag{58}$$

$$\boldsymbol{\Omega}_i = \begin{pmatrix} \mathbb{C}\mathrm{ov}\{\tilde{\boldsymbol{y}}|\mathcal{H}_i\} & \mathrm{p}\mathbb{C}\mathrm{ov}\{\tilde{\boldsymbol{y}}|\mathcal{H}_i\} \\ \mathrm{p}\mathbb{C}\mathrm{ov}\{\tilde{\boldsymbol{y}}|\mathcal{H}_i\}^* & \mathbb{C}\mathrm{ov}\{\tilde{\boldsymbol{y}}|\mathcal{H}_i\}^* \end{pmatrix} = \begin{pmatrix} \boldsymbol{\Omega}_i & \boldsymbol{\Upsilon}_i \\ \boldsymbol{\Upsilon}_i^* & \boldsymbol{\Omega}_i^* \end{pmatrix}. \tag{59}$$

When replacing $\boldsymbol{y}$ with $\boldsymbol{y}$, it is worth noticing that the factor $1/\sqrt{K}$ (resp. $1/K$) in optimal (resp. energy) test does not affect the ROC performance as it can be absorbed in the threshold (γ).

A. Large-System Optimal Test

Exploiting the results in [28] (Chapter 7), the optimal test for large-system scenarios is obtained through the following statistic

$$\lambda = (\boldsymbol{y}-\boldsymbol{\mu}_0)^\dagger\boldsymbol{\Omega}_0^{-1}(\boldsymbol{y}-\boldsymbol{\mu}_0) - (\boldsymbol{y}-\boldsymbol{\mu}_1)^\dagger\boldsymbol{\Omega}_1^{-1}(\boldsymbol{y}-\boldsymbol{\mu}_1), \tag{60}$$

which, by completing the square and absorbing the constant term into the threshold, can be rewritten as the quadratic form

$$\lambda = \frac{1}{2}(\boldsymbol{y}-\boldsymbol{v})^\dagger\boldsymbol{G}(\boldsymbol{y}-\boldsymbol{v}), \tag{61}$$

where we have denoted

$$\boldsymbol{G} = \boldsymbol{\Omega}_0^{-1} - \boldsymbol{\Omega}_1^{-1}, \tag{62}$$

$$\boldsymbol{v} = -\boldsymbol{G}^{-1}\left(\boldsymbol{\Omega}_1^{-1}\boldsymbol{\mu}_1 - \boldsymbol{\Omega}_0^{-1}\boldsymbol{\mu}_0\right). \tag{63}$$

Combining Theorem 1 with (61), we get the following CF

$$\phi_{\lambda|\mathcal{H}_i}(\tau) = \frac{\exp\left(-\frac{1}{2}\boldsymbol{u}_i^\dagger\boldsymbol{\Omega}_i^{-1}\left(\boldsymbol{I}_{2N} - (\boldsymbol{I}_{2N} - j\tau\boldsymbol{\Omega}_i\boldsymbol{G})^{-1}\right)\boldsymbol{u}_i\right)}{\det^{1/2}(\boldsymbol{I}_{2N} - j\tau\boldsymbol{\Omega}_i\boldsymbol{G})}, \tag{64}$$

where we have denoted $\boldsymbol{u}_i = \boldsymbol{\mu}_i - \boldsymbol{v}$. The CF may be used to compute efficiently the CCDF $\Pr(\lambda > \gamma|\mathcal{H}_i)$ using the Gauss-Chebyshev quadrature formulas as done in [6], [12], and [33].

B. Large-System Energy Test

Exploiting both Theorem 1 and the augmented representation in (57), the CF of the received energy $\lambda = \frac{1}{2}\|\boldsymbol{y}\|^2$ for large-system scenarios is obtained replacing $\boldsymbol{G} = \boldsymbol{I}_{2N}$ and $\boldsymbol{v} = \boldsymbol{0}_{2N}$ in (64), i.e.

$$\phi_{\lambda|\mathcal{H}_i}(\tau) = \frac{\exp\left(-\frac{1}{2}\boldsymbol{\mu}_i^\dagger\boldsymbol{\Omega}_i^{-1}\left(\boldsymbol{I}_{2N} - (\boldsymbol{I}_{2N} - j\tau\boldsymbol{\Omega}_i)^{-1}\right)\boldsymbol{\mu}_i\right)}{\det^{1/2}(\boldsymbol{I}_{2N} - j\tau\boldsymbol{\Omega}_i)}. \tag{65}$$

It is worth noticing that the computational complexity for evaluating the exact performance is approximately $O(K^M)$, the number of products in (39) is $\sum_{\ell=0}^{K}(L(\ell)+1)$, while the computational complexity for evaluating the asymptotic performance is approximately $O(N^3)$, the matrix inversion in (65) dominates the complexity. For large-system scenarios, the advantage in using the asymptotic analysis is apparent.

VI. SIMULATION RESULTS

Numerical results refer to Monte Carlo simulations with 10^5 runs using MATLAB. When evaluating the exact performance, we considered WSNs with $K \in \{5, 10\}$ sensors, whose local performance are $(p_f, p_d) = (0.05, 0.5)$, and a FC with $N \in \{1, 2, 4\}$ receiving antennas. On the other hand, when evaluating the large-system approximations, we considered WSNs with $K \in \{50, 100\}$ sensors, whose local performance are $(p_f, p_d) = (0.3, 0.5)$, and a FC with $N = 2$ receiving antennas. A source with equiprobable hypotheses ($\pi_0 = \pi_1 = 1/2$) is assumed.

For Rice fading and 2ZM fading, we characterize the channels with respect to two parameters: (i) the ratio between the (average) power of the two components[2] (denoted ξ); (ii) the average total power (denoted ζ). In the case of NZZ fading we characterize the channel with respect to three parameters by replacing the parameter ξ with parameters ξ_1 and ξ_2 denoting the ratios between the (average) power of the *line-of-sight* component and of the two *non-line-of-sight* components. More specifically, in the case of Rice fading they are

$$\xi = \frac{\|\boldsymbol{\mu}_1\|^2}{\sigma_1^2}, \quad \zeta = \|\boldsymbol{\mu}_1\|^2 + \sigma_1^2, \tag{66}$$

while in the case of 2ZM fading

$$\xi = \frac{\rho_1 \sigma_1^2}{\rho_2 \sigma_2^2}, \quad \zeta = \rho_1 \sigma_1^2 + \rho_2 \sigma_2^2, \tag{67}$$

and finally in the case of NZZ fading

$$\xi_1 = \frac{\|\boldsymbol{\mu}_1\|^2}{\sigma_1^2}, \quad \xi_2 = \frac{\rho_1 \|\boldsymbol{\mu}_1\|^2}{\rho_2 \sigma_2^2},$$
$$\zeta = \rho_1 \|\boldsymbol{\mu}_1\|^2 + \rho_1 \sigma_1^2 + \rho_2 \sigma_2^2. \tag{68}$$

ROC curves are labeled with respect to the received SNR defined as ζ/σ_w^2. Also: (i) only channels with unitary average power will be considered, i.e. $\zeta = 1$; (ii) in the case of 2ZM fading and NZZ fading we will assume equally probable components (i.e. $\rho_1 = \rho_2 = 1/2$); (iii) in the case of Rice fading and NZZ fading we will assume that the mean vector is given by $\boldsymbol{\mu}_1 = \|\boldsymbol{\mu}_1\| \cdot \boldsymbol{a}(\theta)$, where

$$\boldsymbol{a}(\theta) = \frac{1}{\sqrt{N}} (1, e^{j\pi \cos(\theta)}, \ldots, e^{j\pi (N-1) \cos(\theta)})^t, \tag{69}$$

is a normalized steering vector from a source in the far field, and (unless differently specified) we employ $\theta = \pi/6$.

Fig. 2 shows the PDF of the generic (modulus) channel gain for Rice fading, 2ZM fading and NZZ fading with different parameters. It is apparent how:

- increasing ξ makes the statistics more concentrated about the unit in the case of Rice fading;
- increasing ξ makes the statistics more L-shaped with a peak close to zero in the case of 2ZM fading;
- increasing ξ_2 makes the statistics with two more pronounced peaks (one being close to zero) in the case of NZZ fading.

Also, it is worth mentioning that the Rayleigh fading (in which the energy detector is the optimal receiver) is represented by Rice fading with $\xi = 0$ and by 2ZM fading with $\xi = 1$ ($\rho_1 = \rho_2 = 1/2$).

[2]In the case of Rice fading, the two components refer to the *line-of-sight* component (represented by the nonzero mean) and to the *non-line-of-sight* component (represented by the Gaussian-shaped random scattering). In the case of 2ZM fading, the two components refer to the two zero-mean components of the GM.

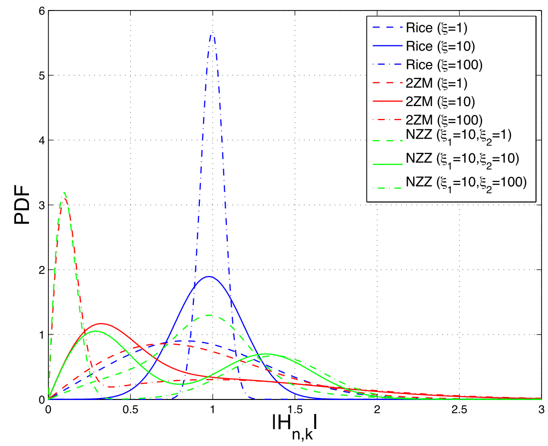

Fig. 2. Impact of ξ, ξ_1 and ξ_2 on the PDF of $|H_{n,k}|$.

A. Analysis and Validation

Fig. 3 shows the ROC curves for WSNs at SNR$\in \{0, 5\}$ dB in the case of Rice fading, 2ZM fading, and NZZ fading when using the energy test. Solid and dashed lines refer to the analytical expressions, i.e. (40), (41), and (42), while circle and diamond markers refer to numerical simulations; a black asterisk represents the local performance of a single sensor. The improvement with respect to the SNR as well as to the number of sensors (K) is apparent. Additionally, the impact of the fading statistics is reflected through the different shape of the ROC curves. Differently, an increase in the number of receive antennas (N) at the FC does not provide necessarily an advantage, and could lead even to performance degradation (e.g. refer to the case with Rice fading at SNR $= 0$ dB). However, concerning this last phenomenon, the following considerations must be noticed: (i) the effect is manly due to the fact that we are considering scenarios with a *line-of-sight* component which is much stronger than the *non-line-of-sight* component and also that, for simplicity though unrealistic, all sensors have the same steering vector $\boldsymbol{a}(\theta)$; (ii) here we are considering a normalized received SNR per antenna (e.g. the normalization factor $1/\sqrt{N}$ in the steering vector $\boldsymbol{a}(\theta)$), thus we are describing only the effect of diversity from multiple receiving antennas while removing the effect of the increased received SNR that in practice will be experienced when adding receiving antennas.

Fig. 4 shows the performance gap between the energy test (solid lines) and the optimal test (dashed lines) for systems at SNR $= 0$ dB in the case of Rice fading, 2ZM fading, and NZZ fading. As analyzed in [16], the energy test performs almost as the optimal test in the case in which all the components of the GM have zero mean. The presence of at least one non-zero-mean component makes the energy test suboptimal. However, the gap between the two tests is very limited, thus making the energy test very appealing considering its simplicity.

Fig. 5 shows the accuracy of the asymptotic performance evaluation, i.e. (65), with respect to the exact analytical expressions for WSNs with $K = 50$ and $K = 100$ sensors whose local performance are $(p_f, p_d) = (0.3, 0.5)$ in the case of Rice

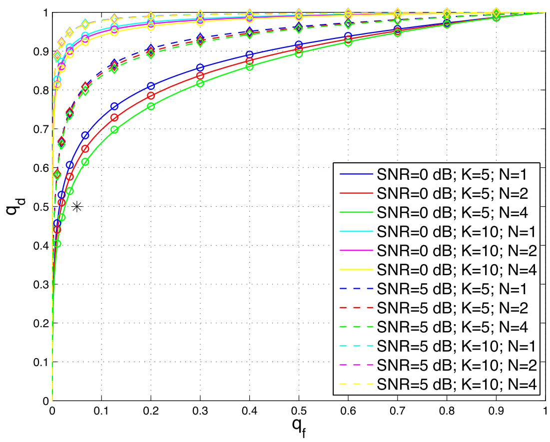

(a) Rice ($\xi = 10$) fading.

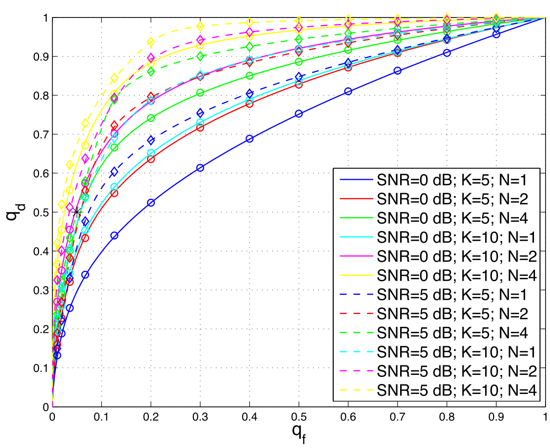

(b) 2ZM ($\xi = 10$) fading.

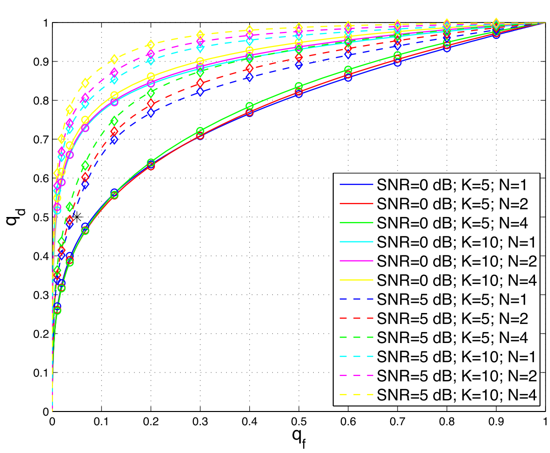

(c) NZZ ($\xi_1 = 10$, $\xi_2 = 10$) fading.

Fig. 3. ROC performance of the energy test. Lines and markers refer to analytical results and numerical simulations. The black asterisk denotes the local performance.

fading, 2ZM fading, and NZZ fading. Also, the asymptotic performance of optimal test are shown: it is apparent how the energy test approaches optimal performance for large-system scenarios.

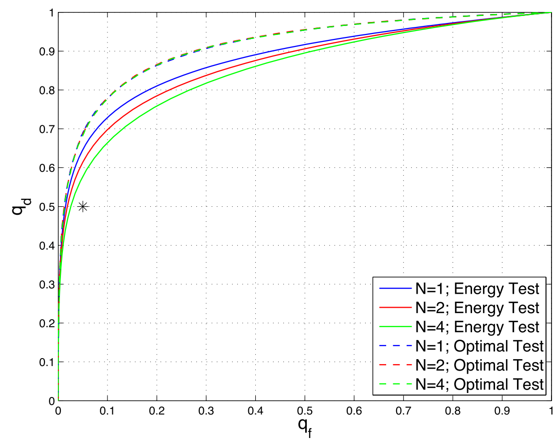

(a) Rice ($\xi = 10$) fading.

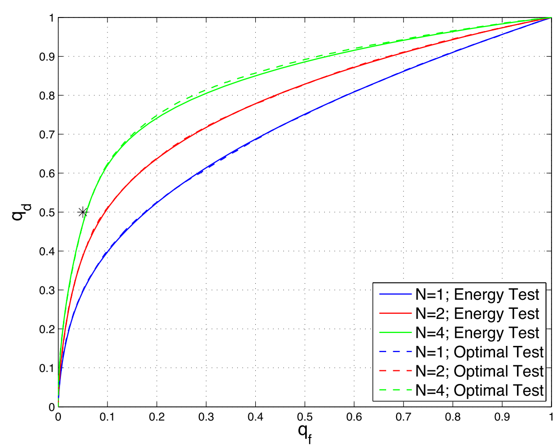

(b) 2ZM ($\xi = 10$) fading.

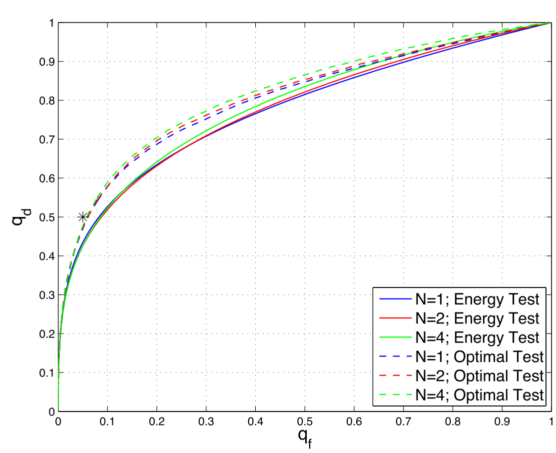

(c) NZZ ($\xi_1 = 10$, $\xi_2 = 10$) fading.

Fig. 4. Gap between the energy and the optimal tests. Systems the FC operating at SNR = 0 dB and $K = 5$ sensors with local performance $(p_f, p_d) = (0.05, 0.5)$.

B. Application: An Example With Random Sensor Distribution

Finally, we present here a further example of the generality of the proposed fading model and corresponding developed analysis.

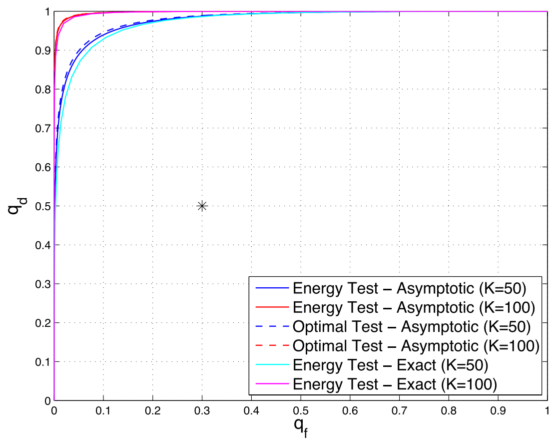

(a) Rice ($\xi = 10$) fading.

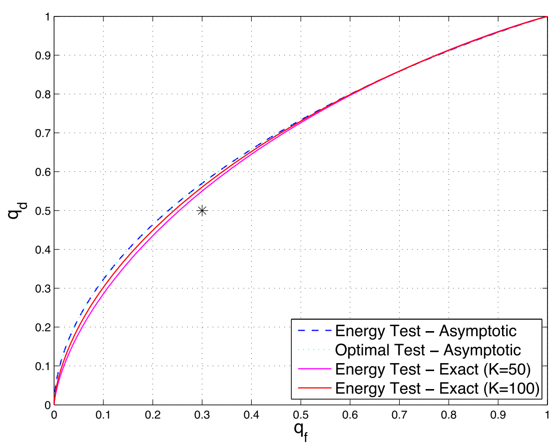

(b) 2ZM ($\xi = 10$) fading.

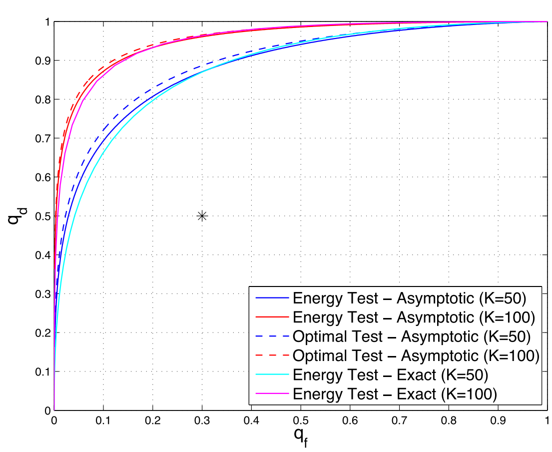

(c) NZZ ($\xi_1 = 10$, $\xi_2 = 10$) fading.

Fig. 5. Asymptotic performance of the energy and the optimal tests. Systems with $N = 2$ receive antenna at the FC and sensor local performance $(p_f, p_d) = (0.3, 0.5)$.

We consider a scenario in which $K \in \{5,\ 10\}$ sensors are *randomly* located at a fixed distance from the FC (or employ power control techniques), equipped with $N = 2$ receiving antennas, within a given angular sector whose width is $\Delta\theta = \pi/2$. The kth sensor undergoes a Rice-fading channel with unitary average power (i.e. $\zeta = 1$), ratio between the *line-of-sight* and *non-line-of-sight* components $\xi = 10$, and steering vector $\boldsymbol{a}(\theta_k)$, where θ_k denotes the *angle-of-arrival* of the kth sensor. Angle of arrivals are assumed to be uniformly distributed within the angular sector. In other words, the generic sensor undergoes a channel vector drawn from the conditional (given the location θ) distribution

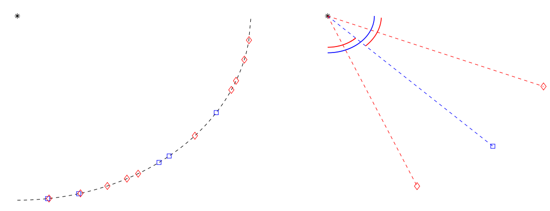

(a) (b)

Fig. 6. Realistic scenario and equivalent models. (a) Blue squares and red diamonds represent possible realizations for $K = 5$ and $K = 10$ sensor locations, respectively. The black asterisk represent the location of the FC. (b) Blue and red solid lines represent the quantized angular domains for equivalent models with $M = 1$ and $M = 2$ components, respectively. Dashed lines and markers represent the corresponding mean vectors.

$$\boldsymbol{h}_{(k)}|\theta \sim \mathcal{N}_{\mathbb{C}}\left(\sqrt{\frac{\xi\zeta}{\xi+1}}\boldsymbol{a}(\theta);\ \frac{\zeta}{\xi+1}\boldsymbol{I}_N\right), \tag{70}$$

where the location θ is uniformly distributed within $[0, \pi/2]$.

We considered the average performance of such a scenario, meaning performance averaged on different random realizations for the location of the sensors. However, due to the ergodicity of the process, the performance of a single realization for the sensors location is representative for the average performance (when the number of sensors is sufficiently large). Additionally, numerical simulations (not reported here for brevity) showed a negligible gap between the performance of a single realization and the average performance even in the case with $K = 5$ sensors.

We then approximate the average performance of such a scenario with the analytical performance given by an equivalent model which exploits a partition of the localization domain and corresponding sample positions. Due to the location probability distribution with fixed distances and uniform angle of arrivals, we use a GM channel with equally-probable components (i.e. $\rho_m = 1/M$), with equal mean-vector norm and equal variance for each component (i.e. $\|\boldsymbol{\mu}_m\| = \mu$ and $\sigma_m^2 = \sigma^2$) chosen in order to enforce unitary average power and ratio between the *line-of-sight* and *non-line-of-sight* components equal to ξ. More specifically, the considered equivalent GM model is distributed according to

$$\boldsymbol{h}_{(k)} \sim \sum_{m=1}^{M} \frac{1}{M}\mathcal{N}_{\mathbb{C}}\left(\sqrt{\frac{\xi\zeta}{\xi+1}}\boldsymbol{a}(\theta_m);\ \frac{\zeta}{\xi+1}\boldsymbol{I}_N\right), \tag{71}$$

where the *angles-of-arrival* are chosen in order to sample in a symmetric way the angular sector, i.e.

$$\theta_m = \frac{(2m-1)}{2M}\Delta\theta, \quad m = 1, \dots, M. \tag{72}$$

Fig. 6 depicts the simulation scenario and the equivalent models with $M \in \{1,\ 2\}$ components. Fig. 7 shows the performance of the scenario obtained through numerical simulations

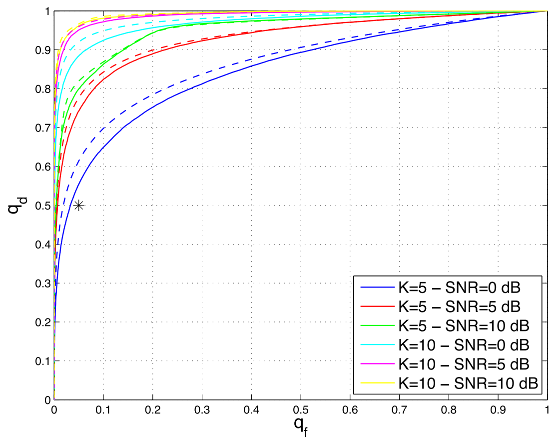

(a) Equivalent model with $M = 1$ component.

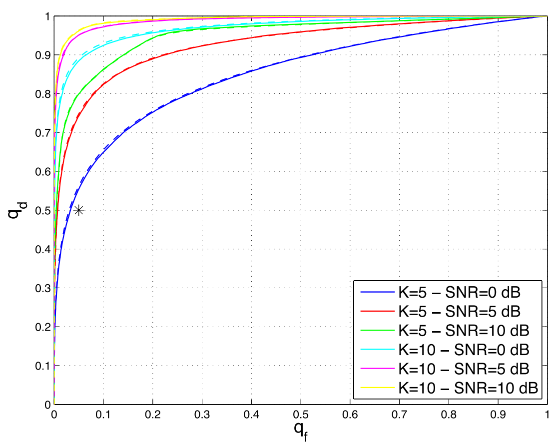

(b) Equivalent model with $M = 2$ components.

Fig. 7. ROC curves for energy test in a realistic scenario with $N = 2$ receiving antennas at the FC. Solid and dashed lines refer to the performance of the simulation and of the equivalent models, respectively. The black asterisk denotes the local performance.

(solid lines) when SNR$\in \{0,\ 5,\ 10\}$ dB, and the corresponding analytical performance obtained through the GM model (dashed lines). It is apparent how in this simple scenario, the model with $M = 1$ component has a small mismatch with the real performance, while the model with $M = 2$ components is able to describe with high accuracy the real performance. It is apparent how a general GM model would be able to describe accurately the average performance of a more sophisticated scenario with range-dependent channel models by choosing the components as an appropriate sampling of the angular-range domain.

VII. Conclusion

We analyzed energy and optimal tests for distributed binary detection by using a WSN connected through a virtual MIMO reporting channel to FC equipped with multiple antennas. GM models have been considered in order to deal with arbitrary fading scenarios. Exact analytical performance are derived and verified for the energy test. Comparison between the energy and the optimal tests were provided. Asymptotic analysis was developed for both energy and optimal tests showing the optimality of the energy test in large-system scenarios. A final example to demonstrate how the work developed here may be used to characterize realistic scenarios was provided.

Acknowledgment

The authors would like to thank the Associate Editor and the anonymous reviewers for dedicating their time to the final version of this manuscript.

Appendix A
CF of the Quadratic Form of an Improper Gaussian

Define the transformation matrix $\boldsymbol{T}$ as

$$\boldsymbol{T} = \begin{pmatrix} \boldsymbol{I}_N & j\boldsymbol{I}_N \\ \boldsymbol{I}_N & -j\boldsymbol{I}_N \end{pmatrix}, \tag{73}$$

and notice that $\boldsymbol{T}\boldsymbol{T}^\dagger = \boldsymbol{T}^\dagger\boldsymbol{T} = 2\boldsymbol{I}_{2N}$. Denoting $\boldsymbol{u} = \Re\{\boldsymbol{x}\}$ and $\boldsymbol{v} = \Im\{\boldsymbol{x}\}$, then $\boldsymbol{z} = \left(\boldsymbol{u}^t, \boldsymbol{v}^t\right)^t$ is the real-composite representation of the vector $\boldsymbol{x}$. Augmented and real-composite descriptions are linked through the following equations [28]

$$\boldsymbol{z} = \frac{1}{2}\boldsymbol{T}^\dagger\boldsymbol{x}, \tag{74}$$

$$\boldsymbol{\mu}_z = \mathbb{E}\{\boldsymbol{z}\} = \frac{1}{2}\boldsymbol{T}^\dagger\boldsymbol{\mu}, \tag{75}$$

$$\boldsymbol{\Omega}_z = \mathbb{C}\text{ov}\{\boldsymbol{z}\} = \frac{1}{4}\boldsymbol{T}^\dagger\boldsymbol{\Omega}\boldsymbol{T}, \tag{76}$$

while the quadratic form may be expressed as $y = \frac{1}{2}\boldsymbol{x}^\dagger\boldsymbol{A}\boldsymbol{x} = \boldsymbol{z}^t\boldsymbol{B}\boldsymbol{z}$ with $\boldsymbol{B} = \frac{1}{2}\boldsymbol{T}^\dagger\boldsymbol{A}\boldsymbol{T}$. The CF of a quadratic form of a real-valued Gaussian random vector is found in [38], then

$$\phi_y(\tau) = \frac{\exp\left(-\frac{1}{2}\boldsymbol{\mu}_z^t\boldsymbol{\Omega}_z^{-1}\left(\boldsymbol{I}_{2N} - (\boldsymbol{I}_{2N} - j2\tau\boldsymbol{\Omega}_z\boldsymbol{B})^{-1}\right)\boldsymbol{\mu}_z\right)}{\det^{1/2}(\boldsymbol{I}_{2N} - j2\tau\boldsymbol{\Omega}_z\boldsymbol{B})}. \tag{77}$$

Using some matrix manipulations we may replace

$$\boldsymbol{\Omega}_z^{-1}\boldsymbol{\mu}_z = \boldsymbol{T}^\dagger\boldsymbol{\Omega}^{-1}\boldsymbol{\mu}, \tag{78}$$

$$\boldsymbol{\Omega}_z\boldsymbol{B} = \frac{1}{4}\boldsymbol{T}^\dagger\boldsymbol{\Omega}\ \boldsymbol{A}\boldsymbol{T}, \tag{79}$$

into (77). Then, exploiting the properties of the transformation matrix $\boldsymbol{T}$ and Sylvester's determinant theorem, we can write (80) and (81) at the bottom of this page, which easily lead to the expression in (17).

$$\boldsymbol{T}\left(\boldsymbol{I}_{2N} - \left(\boldsymbol{I}_{2N} - j\frac{\tau}{2}\boldsymbol{T}^\dagger\boldsymbol{\Omega}\ \boldsymbol{A}\boldsymbol{T}\right)^{-1}\right)\boldsymbol{T}^\dagger = 2\left(\boldsymbol{I}_{2N} - (\boldsymbol{I}_{2N} - j\tau\boldsymbol{\Omega}\ \boldsymbol{A})^{-1}\right), \tag{80}$$

$$\det\left(\boldsymbol{I}_{2N} - j\frac{\tau}{2}\boldsymbol{T}^\dagger\boldsymbol{\Omega}\ \boldsymbol{A}\boldsymbol{T}\right) = \det\left(\boldsymbol{I}_{2N} - j\tau\boldsymbol{\Omega}\ \boldsymbol{A}\right). \tag{81}$$

APPENDIX B
SECOND-ORDER CHARACTERIZATION OF THE RECEIVED SIGNAL

Let us denote $\boldsymbol{\xi}_{(k)} = \boldsymbol{h}_{(k)} x_k$ and $\boldsymbol{\xi} = \sum_{k=1}^{K} \boldsymbol{\xi}_{(k)}$, it is apparent that

$$\begin{aligned}\mathbb{E}\left\{\boldsymbol{\xi}_{(k)}|\mathcal{H}_i\right\} &= \mathbb{E}\left\{\boldsymbol{h}_{(k)}|\mathcal{H}_i\right\}\mathbb{E}\{x_k|\mathcal{H}_i\}\\ &= p_{i,k}\boldsymbol{\mu}_H, \end{aligned}\tag{82}$$

$$\begin{aligned}\mathbb{E}\left\{\boldsymbol{\xi}_{(k)}\boldsymbol{\xi}_{(k)}^{\dagger}|\mathcal{H}_i\right\} &= \mathbb{E}\left\{\boldsymbol{h}_{(k)}\boldsymbol{h}_{(k)}^{\dagger}|\mathcal{H}_i\right\}\mathbb{E}\left\{x_k^2|\mathcal{H}_i\right\}\\ &= p_{i,k}\boldsymbol{R}_H, \end{aligned}\tag{83}$$

$$\begin{aligned}\mathbb{E}\left\{\boldsymbol{\xi}_{(k)}\boldsymbol{\xi}_{(k)}^{t}|\mathcal{H}_i\right\} &= \mathbb{E}\left\{\boldsymbol{h}_{(k)}\boldsymbol{h}_{(k)}^{t}|\mathcal{H}_i\right\}\mathbb{E}\left\{x_k^2|\mathcal{H}_i\right\}\\ &= p_{i,k}\boldsymbol{Q}_H, \end{aligned}\tag{84}$$

and then

$$\mathbb{C}\mathrm{ov}\{\boldsymbol{\xi}_{(k)}|\mathcal{H}_i\} = p_{i,k}\left(\boldsymbol{R}_H - p_{i,k}\boldsymbol{\mu}_H\boldsymbol{\mu}_H^{\dagger}\right), \tag{85}$$

$$\mathrm{p}\mathbb{C}\mathrm{ov}\{\boldsymbol{\xi}_{(k)}|\mathcal{H}_i\} = p_{i,k}\left(\boldsymbol{Q}_H - p_{i,k}\boldsymbol{\mu}_H\boldsymbol{\mu}_H^{t}\right), \tag{86}$$

Noticing that $\boldsymbol{y} = \boldsymbol{\xi} + \boldsymbol{w}$, then it is straightforward to get Eqs. (43), (44), and (45).

REFERENCES

[1] P. K. Varshney, *Distributed Detection and Data Fusion*. New York, NY, USA: Springer, 1997.

[2] B. Chen, L. Tong, and P. K. Varshney, "Channel-aware distributed detection in wireless sensor networks," *IEEE Signal Process. Mag.*, vol. 23, no. 4, pp. 16–26, Jul. 2006.

[3] A. G. Dimakis, S. Kar, J. M. F. Moura, M. G. Rabbat, and A. Scaglione, "Gossip algorithms for distributed signal processing," *Proc. IEEE*, vol. 98, no. 11, pp. 1847–1864, Nov. 2010.

[4] B. Chen, R. Jiang, T. Kasetkasem, and P. K. Varshney, "Channel aware decision fusion in wireless sensor networks," *IEEE Trans. Signal Process.*, vol. 52, no. 12, pp. 3454–3458, Dec. 2004.

[5] S. Laitrakun and E. J. Coyle, "Reliability-based splitting algorithms for time-constrained distributed detection in random-access WSNs," *IEEE Trans. Signal Process.*, vol. 62, no. 21, pp. 5536–5551, Nov. 2014.

[6] A. Lei and R. Schober, "Coherent max-log decision fusion in wireless sensor networks," *IEEE Trans. Commun.*, vol. 58, no. 5, pp. 1327–1332, May 2010.

[7] A. Lei and R. Schober, "Multiple-symbol differential decision fusion for mobile wireless sensor networks," *IEEE Trans. Wireless Commun.*, vol. 9, no. 2, pp. 778–790, Feb. 2010.

[8] C. R. Berger, M. Guerriero, S. Zhou, and P. Willett, "PAC vs. MAC for decentralized detection using noncoherent modulation," *IEEE Trans. Signal Process.*, vol. 57, no. 9, pp. 3562–3575, Sep. 2009.

[9] F. Li, J. S. Evans, and S. Dey, "Decision fusion over noncoherent fading multiaccess channels," *IEEE Trans. Signal Process.*, vol. 59, no. 9, pp. 4367–4380, Sep. 2011.

[10] M. K. Banavar, A. D. Smith, C. Tepedelenlioglu, and A. Spanias, "On the effectiveness of multiple antennas in distributed detection over fading MACs," *IEEE Trans. Wireless Commun.*, vol. 11, no. 5, pp. 1744–1752, May 2012.

[11] D. Ciuonzo, G. Romano, and P. Salvo Rossi, "Channel-aware decision fusion in distributed MIMO wireless sensor networks: Decode-and-fuse vs. decode-then-fuse," *IEEE Trans. Wireless Commun.*, vol. 11, no. 8, pp. 2976–2985, Aug. 2012.

[12] D. Ciuonzo, G. Romano, and P. Salvo Rossi, "Performance analysis and design of maximum ratio combining in channel-aware MIMO decision fusion," *IEEE Trans. Wireless Commun.*, vol. 12, no. 9, pp. 4716–4728, Sep. 2013.

[13] D. Ciuonzo, P. Salvo Rossi, and S. Dey, "Massive MIMO channel-aware decision fusion," *IEEE Trans. Signal Process.*, vol. 63, no. 3, pp. 604–619, Feb. 2015.

[14] C. Rago, P. Willett, and Y. Bar-Shalom, "Censoring sensors: A low-communication-rate scheme for distributed detection," *IEEE Trans. Aerosp. Electron. Syst.*, vol. 32, no. 2, pp. 554–568, Apr. 1996.

[15] D. Ciuonzo, G. Romano, and P. Salvo Rossi, "Optimality of received energy in decision fusion over Rayleigh fading diversity MAC with non-identical sensors," *IEEE Trans. Signal Process.*, vol. 61, no. 1, pp. 22–27, Jan. 2013.

[16] P. Salvo Rossi, D. Ciuonzo, K. Kansanen, and T. Ekman, "On energy detection for MIMO decision fusion in wireless sensor networks over NLOS fading," *IEEE Commun. Lett.*, vol. 19, no. 2, pp. 303–306, Feb. 2015.

[17] P. Salvo Rossi, D. Ciuonzo, T. Ekman, and H. Dong, "Energy detection for MIMO decision fusion in underwater sensor networks," *IEEE Sensors J.*, vol. 15, no. 3, pp. 1630–1640, Mar. 2015.

[18] P. Salvo Rossi, D. Ciuonzo, and T. Ekman, "HMM-based decision fusion in wireless sensor networks with noncoherent multiple access," *IEEE Commun. Lett.*, vol. 19, no. 5, pp. 871–874, May 2015.

[19] J. T. Flåm, S. Chatterjee, K. Kansanen, and T. Ekman, "On MMSE estimation: A linear model under Gaussian mixture statistics," *IEEE Trans. Signal Process.*, vol. 60, no. 7, pp. 3840–3845, Jul. 2012.

[20] B. Selim, O. Alhussein, S. Muhaidat, G. K. Karagiannidis, and J. Liang, "Modeling and analysis of wireless channels via the mixture of Gaussian distribution," *IEEE Trans. Veh. Technol.*, 2015, to be published.

[21] B. Selim, O. Alhussein, G. K. Karagiannidis, and S. Muhaidat, "Optimal cooperative spectrum sensing over composite fading channels," in *Proc. IEEE Int. Conf. Commun.*, Jun. 2015, pp. 520–525.

[22] T. Olofsson, A. Ahlén, and M. Gidlund, "Modeling of the fading statistics of wireless sensor network channels in industrial environments," *IEEE Trans. Signal Process.*, vol. 64, no. 12, pp. 3021–3034, Jun. 2016.

[23] P. Salvo Rossi, D. Ciuonzo, T. Ekman, and K. Kansanen, "Energy detection for decision fusion in wireless sensor networks over Ricean-mixture fading," in *Proc. IEEE Sensor Array Multichannel Signal Process. Workshop (SAM)*, Jun. 2014, pp. 265–268.

[24] A. Papoulis and S. U. Pillai, *Probability, Random Variables and Stochastic Processes*. New York, NY, USA: McGraw-Hill, 2002.

[25] W. H. Greene, *Econometric Analysis*. Englewood Cliffs, NJ, USA: Prentice-Hall, 2007.

[26] G. L. Turin, "The characteristic function of Hermitian quadratic forms in complex normal variables," *Biometrika*, vol. 47, nos. 1–2, pp. 199–201, Jun. 1960.

[27] M. K. Simon, *Probability Distributions Involving Gaussian Random Variables*. New York, NY, USA: Springer, 2002.

[28] P. J. Schreier and L. L. Scharf, *Statistical Signal Processing of Complex-Valued Data: The Theory of Improper and Noncircular Signals*. Cambridge, U.K.: Cambridge Univ. Press, 2010.

[29] Y. Sung, L. Tong, and A. Swami, "Asymptotic locally optimal detector for large-scale sensor networks under the Poisson regime," *IEEE Trans. Signal Process.*, vol. 53, no. 6, pp. 2005–2017, Jun. 2005.

[30] M. Guerriero, L. Svensson, and P. Willett, "Bayesian data fusion for distributed target detection in sensor networks," *IEEE Trans. Signal Process.*, vol. 58, no. 6, pp. 3417–3421, Jun. 2010.

[31] S. M. Kay, *Fundamentals of Statistical Signal Processing: Detection Theory*, vol. 2. Englewood Cliffs, NJ, USA: Prentice-Hall, 1998.

[32] M. Fernandez and S. Williams, "Closed-form expression for the Poisson-binomial probability density function," *IEEE Trans. Aerosp. Electron. Syst.*, vol. 46, no. 2, pp. 803–817, Apr. 2010.

[33] P. Salvo Rossi, D. Ciuonzo, and G. Romano, "Orthogonality and cooperation in collaborative spectrum sensing through MIMO decision fusion," *IEEE Trans. Wireless Commun.*, vol. 12, no. 11, pp. 5826–5836, Nov. 2013.

[34] F. F. Digham, M.-S. Alouini, and M. K. Simon, "On the energy detection of unknown signals over fading channels," *IEEE Trans. Commun.*, vol. 55, no. 1, pp. 21–24, Jan. 2007.

[35] V. M. Kapinas, S. K. Mihos, and G. K. Karagiannidis, "On the monotonicity of the generalized Marcum and Nuttall Q-functions," *IEEE Trans. Inf. Theory*, vol. 55, no. 8, pp. 3701–3710, Aug. 2009.

[36] I. Nevat, G. W. Peters, and I. B. Collings, "Distributed detection in sensor networks over fading channels with multiple antennas at the fusion centre," *IEEE Trans. Signal Process.*, vol. 62, no. 3, pp. 671–683, Feb. 2014.

[37] F. Jiang, J. Chen, A. L. Swindlehurst, and J. A. López-Salcedo, "Massive MIMO for wireless sensing with a coherent multiple access channel," *IEEE Trans. Signal Process.*, vol. 63, no. 12, pp. 3005–3017, Jun. 2015.

[38] J. K. Thomas, L. L. Scharf, and D. W. Tufts, "The probability of a subspace swap in the SVD," *IEEE Trans. Signal Process.*, vol. 43, no. 3, pp. 730–736, Mar. 1995.

Pierluigi Salvo Rossi (SM'11) was born in Naples, Italy, in 1977. He received the Laurea (*summa cum laude*) degree in telecommunications engineering and the Ph.D. degree in computer engineering from the University of Naples Federico II, Naples, Italy, in 2002 and 2005, respectively. He has been a Researcher with the Inter-Departmental Research Center for Signals Analysis and Synthesis, University of Naples Federico II, the Department of Information Engineering, Second University of Naples, Aversa, Italy, the Communications and Signal Processing Laboratory, and the Department of Electrical and Computer Engineering, Drexel University, Philadelphia, PA, USA, and an Adjunct Professor with the Faculty of Engineering, Second University of Naples. From 2005 to 2008 he held a post-doctoral position with the Department of Computer Science and Systems, University of Naples Federico II, the Department of Information Engineering, Second University of Naples, and the Department of Electronics and Telecommunications, Norwegian University of Science and Technology, Trondheim, Norway, and visited the Department of Electrical and Information Technology, Lund University, Lund, Sweden. From 2008 to 2014, he was an Assistant Professor (tenured in 2011) in telecommunications with the Department of Industrial and Information Engineering, Second University of Naples, and visited the Department of Electronics and Telecommunications, Norwegian University of Science and Technology, and the Excellence Center for Wireless Sensor Networks, Uppsala University, Uppsala, Sweden. Since 2014, he has been, first, an Associate Professor and then a Professor in signal processing with the Department of Electronics and Telecommunications, Norwegian University of Science and Technology. He was an Associate Editor of the IEEE COMMUNICATIONS LETTERS from 2012 to 2016 and currently serves as an Associate Editor of the IEEE TRANSACTIONS ON WIRELESS COMMUNICATIONS, and a Senior Editor of the IEEE COMMUNICATIONS LETTERS. His research interests fall within the areas of communications and signal processing.

Domenico Ciuonzo (S'11–M'14–SM'16) received the B.Sc. and M.Sc. (*summa cum laude*) degrees in computer engineering and the Ph.D. degree from the Second University of Naples, Aversa, Italy, in 2007, 2009, and 2013, respectively. In 2011, he was involved in the Visiting Researcher Programme of NATO CMRE, La Spezia, Italy. In 2012, he was a Visiting Scholar with the ECE Department, University of Connecticut, Storrs, CT, USA. In 2015, he held a visiting appointment with the Department of Electronics and Telecommunications, Norwegian University of Science and Technology, Trondheim, Norway. Since 2014, he has been a Post-Doctoral Researcher with DIETI, University of Naples, Federico II, Italy. His research interests are mainly in the areas of data fusion, statistical signal processing, target tracking, and wireless sensor networks. His reviewing activity was recognized by the IEEE COMMUNICATIONS LETTERS and the IEEE TRANSACTIONS ON COMMUNICATIONS, which nominated him Exemplary Reviewer in 2013 and 2014, respectively. Since 2014 he serves as an Associate Editor of the *IEEE Aerospace and Electronic Systems Magazine* and since 2016 he serves as an Associate Editor of the IEEE TRANSACTIONS ON AEROSPACE AND ELECTRONIC SYSTEMS).

Kimmo Kansanen (S'99–M'04) received the M.Sc. degree in EE and the Dr.Tech. degree from the University of Oulu, Finland, in 1998 and 2005, respectively, where he was a Research Scientist and a Project Manager with the Centre for Wireless Communications. He held a post-doctoral position with the Norwegian University of Science and Technology, Trondheim, Norway. Since 2006, he has been a Research Scientist and an Associate Professor with the Norwegian University of Science and Technology. He has been a Professor with the Norwegian University of Science and Technology, since 2016. His research interests are within communications and signal processing. He is currently with the Editorial Board of Elsevier *Physical Communications*.

Torbjörn Ekman (M'02) was born in Västerås, Sweden, in 1969. He received the M.Sc. degree in engineering physics and the Ph.D. degree in signal processing from Uppsala University, Sweden, in 1994 and 2002, respectively. He received the Ph.D. degree in UniK from the University Graduate Center, Kjeller, Norway, in 2005, From 1997 to 1998, he was a Visiting Scientist with the Institute of Communications and Radio-Frequency Engineering, Vienna University of Technology, Vienna, Austria, on a Marie Curie Grant. From 1999 to 2002, he visited the Digital Signal Processing Group, University of Oslo, Norway. In 2006, he joined as an Associate Professor with the Department of Electronics and Telecommunications, Norwegian University of Science and Technology, Trondheim, Norway, where since 2015, he has been a Professor. His current research interests include signal processing in wireless communications, scheduling of radio resources and dynamic modeling, and prediction of radio channels. He is currently participating in projects on broadband radio access and cognitive radio, studying radio resource management, and channel modeling.